Total-atom differential coherent-scattering cross-section measurements on Sn and Pb using moderate-energy γ rays

D. A. Bradley and A. M. Ghose

School of Physics, Universiti Sains Malaysia, Minden, Penang, Malaysia
(Received 29 April 1985)

Accurate, $O(5\%)$ measurements of total-atom differential coherent-scattering cross sections of Sn and Pb within the range of scattering angles $10° < \psi < 60°$ have been performed using 279.2- and 661.6-keV photons and a surface-of-revolution scatterer geometry. Comparison, with the predictions of Kissel, Pratt, and Roy and the various form-factor formulations, reveals general agreement with the predictions of Kissel *et al.* A systematic departure from agreement is apparent, however, at the smallest angle of scattering. Critical examination of other recent measured data also indicates a trend towards poorer agreement at smaller angles.

I. INTRODUCTION

Although the physical mechanisms underlying the processes composing the phenomenon of coherent scattering of x rays and γ rays have been known for a long time, it is only recently that accurate values of the differential cross sections of Rayleigh scattering, which is usually the dominant coherent process for moderate-energy photons, have been available for selected elements and angles of scattering.[1] A few years ago the accuracy of experimental cross-section data[2] usually surpassed that of its theoretical counterparts, but the situation has now been reversed. The present investigations were carried out in an effort to obtain accurately measured atomic differential coherent-scattering cross sections of tin and lead for ^{137}Cs and ^{203}Hg photons. By optimizing geometric factors[3] one is able to reduce or eliminate several sources of error; the known residual errors have also been explicitly calculated so that realistic comparison between experimental and theoretical cross sections may be made.

In the next section we briefly review theoretical calculations of the differential coherent-scattering cross sections within the energy range examined in the present investigations. In the subsequent sections we discuss the "surface-of-revolution" geometry used in the present measurements and analyze in detail the significant sources of error. Differential coherent-scattering cross sections are reported for the elements Sn and Pb within the range of scattering angles 10°–60° for the energies 279.2 and 661.6 keV. Deviations from the predictions of Kissel, Pratt, and Roy[1] as well as the various form-factor formalisms have been analyzed. Corroborative evidence is found in other studies using high-resolution detector systems.

II. THEORETICAL VALUES OF ATOMIC COHERENT-SCATTERING CROSS SECTIONS

For the photons under study the atomic differential coherent-scattering amplitude is obtained, neglecting higher-order processes, by the superposition of the corresponding amplitudes for Rayleigh and nuclear Thomson scattering. The amplitude for Delbrück scattering is only significant for the higher-atomic-number elements at large angles of scattering; this situation was not studied in the investigations reported herein.

Earliest calculations of Rayleigh scattering were carried out under the form-factor approximation in which the binding energy of the electrons is neglected. Tabulated values of the Rayleigh form-factor amplitudes have been computed by Hubbell *et al.* in Refs. 4 and 5 using nonrelativistic and relativistic wave functions, respectively. Franz[6] suggested a modified form factor which took the electron binding effect into account and tabulated[7] values of the modified relativistic form factors are available now.

Brown and co-workers[8–12] developed an exact analytical method for solving the second-order perturbation theory. Due to the enormous computing efforts involved, calculations were restricted to the evaluation of the K-shell contributions of Hg at four discrete energies, viz., $0.32mc^2$, $0.64mc^2$, $1.28mc^2$, and $2.56mc^2$. Cornille and Chapdelaine[13] extended the evaluation to $5.12mc^2$.

Johnson and Feiock[14,15] improved Brown *et al.*'s formalism by use of the more realistic Dirac-Hartree-Fock-Slater (DHFS) wave function. Lin, Cheng, and Johnson[16] included higher-order electron-electron correlation contributions arising from the fourth-order S matrix, which had been neglected in the previous work. Johnson and Cheng[17] used these improvements to calculate Rayleigh scattering for photons of energy 100–900 keV by relatively heavy elements in the range of Z from 30 to 82. Overall discrepancies between experimental and theoretical calculations were now $O(10\%)$ and it was obviously desirable to reduce further the uncertainties in the theoretical calculations.

The desired goal was achieved by Kissel and Pratt,[18] who improved upon the previous investigations in a number of ways. In spite of these improvements the computation of Rayleigh-scattering amplitudes still required a considerable amount of computer time. In view of this a prescription was developed to evaluate the total Rayleigh cross section for any element at any angle of scattering and for photons within an energy range of 100 eV to 10 MeV with an uncertainty of $O(1\%)$ or less, whereby higher-shell contributions are included partly by incor-

poration of the modified relativistic form factors and partly by recourse to the use of ratios of photoeffect amplitudes for inner and outer electron shells.[1]

III. METHOD

A. Scatterer geometry

Two popular scatterer geometries are the annular geometry and the configuration with a plane scatterer positioned on the Thales circle described between the source and detector.[19] In these methods there are problems arising from multiple scattering and absorption in the scatterer and large spread in the definition of the scattering angles. In the present investigation, the scatterer was distributed in the form of a thin incomplete surface of revolution obtained by rotating an arc of a circle passing through the centers of the source and the scatterer. The principal advantage of this arrangement is reduction in the multiple scattering and absorption, without loss in the intensity of the scattered beam. The definition of the an-

gle of scattering is also quite precise in this method. Further, a number of sources of error are either reduced or rendered insignificant due to the symmetry of the arrangement.

B. Counting rate

In the version of the axial symmetry method utilized herein we have used scatterers in the form of strips of constant width and thickness, distributed over a portion of the surface of revolution. The scattered intensity was compared with that of the primary source. Auxiliary sources of intermediate strengths placed at different locations were used to facilitate this comparison as well as to take into account the variation of the effective efficiency of the detector for different parts of the scatterer. The counting rate due to coherent scattering arising from the scatterer is easily obtained from the equations given by Ghose and Bradley,[19] noting that we are using strips rather than a continuous scatterer. Using cylindrical coordinates (r, ψ, z) as shown in Fig. 1 we have

$$N_c = \frac{d\sigma}{d\Omega}(\psi) \left[\frac{N_c^0}{n_c^0} \right] \frac{nw}{2l} \int_{\Sigma} \left[\frac{1 - \exp\left[-v\sigma_t \sec\phi \left[1 + \left| \frac{\cos\phi}{\cos(\phi+\psi)} \right| \right] \right]}{v\sigma_t \left[1 + \left| \frac{\cos\phi}{\cos(\phi+\psi)} \right| \right] \sec\phi} \right]$$

$$\times \frac{(\tan^2\psi)(\sec\psi)n_c dx}{(\sec^2\psi - x^2\tan^2\psi)^{1/2}[\sec^2\psi - x\tan^2\psi - (\sec^2\psi - x^2\tan^2\psi)^{1/2}]} , \quad (1)$$

where N_c is the observed coherent-scattering counting rate arising from the scatterers, N_c^0 is the counting rate obtained from the primary source in the absence of scatterers and shadow bar, n_c^0 is the counting rate obtained from the auxiliary source placed at the primary-source position in the absence of the primary source, scatterers, and shadow bar, and n_c is the counting rate obtained from the auxiliary source placed at various positions over the scattering surface. In addition, $d\sigma(\psi)/d\Omega$ is the differential coherent-scattering cross section obtained at the angle of scattering ψ, n is the number of scattering strips, w is the width of each of the scattering strips, $2l$ is the distance of separation between source and detector, $\int_{\Sigma}$ indicates integration over the whole scatterer

surface, v is the number of scattering centers per unit volume, σ_t is the total scattering cross section for the particular element and energy with t the thickness of the scatterer, $x = z/l$ is the dimensionless axial coordinate, and ϕ is the normal to the scatterer surface as defined in Fig. 1.

Assuming that the limits of the extent of the scatterer are $\pm x_1$, one obtains

$$\frac{d\sigma(\psi)}{d\Omega} = N_c \left[\frac{n_c^0}{N_c^0} \right] \frac{2l}{nw} \frac{1}{f \tan^2\psi \sec\psi} , \quad (2)$$

where

$$f = \int_{-x_1}^{+x_1} \frac{n_c(x)dx}{(\sec^2\psi - x^2\tan^2\psi)^{1/2}[\sec^2\psi + x\tan^2\psi - (\sec^2\psi - x^2\tan^2\psi)^{1/2}]} \frac{1 - \exp\left[-v\sigma_t\sec\phi \left[1 + \left| \frac{\cos\phi}{\cos(\phi+\psi)} \right| \right] \right]}{v\sigma_t \left[1 + \left| \frac{\cos\phi}{\cos(\phi+\psi)} \right| \right] \sec\phi} \quad (3)$$
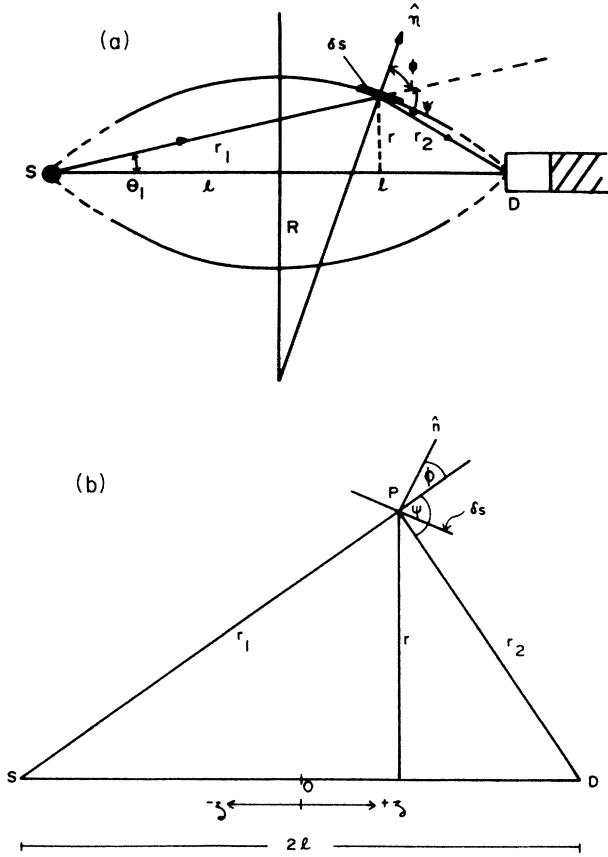
FIG. 1. (a) Surface-of-revolution geometry showing the relative positions of the main source (S), an element of the scatterer surface (δs), and the detector (D). (b) An enlarged view of a portion of the surface-of-revolution geometry.
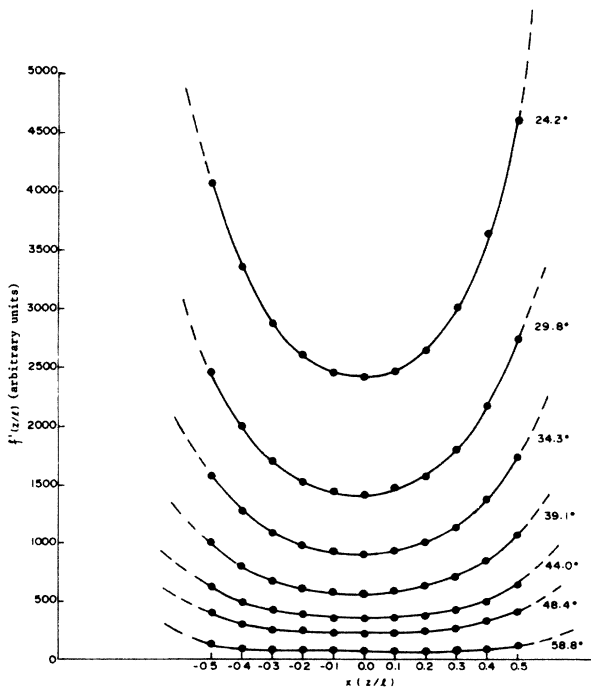

FIG. 2. Variation of the scatterer-dimension- and shape-dependent function $f'(z/l)$ for various scattering angles ψ, corresponding to a source-to-detector separation of 2 m.

is the explicitly scatterer-dimension- and shape-dependent function evaluated by numerical integration. We have examined the variation of the more restrictive shape-dependent function $f'(x)$ where

$$f = \int_{-x_1}^{+x_1} f'(x) \frac{1 - \exp\left[-v\sigma_t \sec\phi \left[1 + \left|\frac{\cos\phi}{\cos(\phi+\psi)}\right|\right]\right]}{v\sigma_t \left[1 + \left|\frac{\cos\phi}{\cos(\phi+\psi)}\right|\right] \sec\phi}.$$

(4)

In the actual experiment x_1 was limited to around ± 0.5 to avoid rapid variation of $f'(x)$ with x for values close to ± 1. In Fig. 2 we have shown this variation for a few typical cases.

C. Multiple scattering

In our experiment we have also limited the thickness of the scatterers to a fraction of the total mean free path, with consequent reduction in the effect of multiple scattering within the absorbers. To estimate the residual effect we have calculated the ratio of the intensity of the coherently scattered beam incident on any area dS_0 arising from other parts of the scatterer to the intensity of the direct beam incident over dS_0. With reference to Fig. 3 it may be seen that this ratio is approximately given by

$$M = \frac{\int_\Sigma d\Omega \frac{t}{\lambda} \sec\phi \frac{d\sigma_{\text{coh}}}{d\Omega}(\theta') d\Omega'}{d\Omega_0 \sigma_t},$$

(5)

where λ is the total mean free path of the incident photon in the scatterer Σ while $d\Omega'$ and $d\Omega_0$ are the solid angles subtended by dS_0 at the scatterer element and at the source position, respectively. $d\sigma_{\text{coh}}(\theta')/d\Omega$ is the differential coherent-scattering cross section for angle θ' where θ' is the angle made by $\mathbf{r}$ with $\mathbf{r}'$. This relationship may be approximated as

$$M = \frac{t}{\lambda} \left\langle \frac{d\sigma_{\text{coh}}}{d\Omega} \frac{\psi - \theta_0}{\sigma_t} \frac{d\Omega'}{d\Omega_0} \right\rangle_{\text{av}} \pi \cos(\psi/2 - \cos\psi).$$
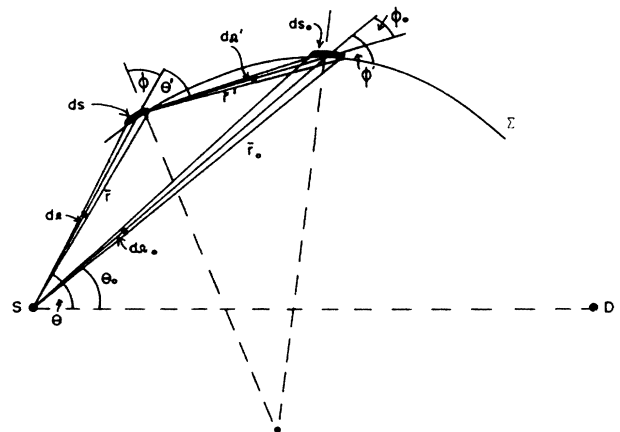
(6)

FIG. 3. Consideration of multiple scattering within a thin but extensive scatterer.

When the angle of scattering is small the last term in the expression determines that M is small, $O(1\%)$ or less. When the angle of scattering is large the averaged term determines that the value of M is very small, with the exception of the case where $d\Omega'$ lies close to $d\Omega_0$; in this case we have the situation of localized scattering within a ring geometry with narrow scatterers. Here it is evident that multiple scattering is negligible. Similar considerations show that multiple scattering involving the shadow bar introduces no appreciable errors in the present measurements.

D. The effect of finite detector and source sizes

Due to the finite size of the detector, the latter detects photons which are not all scattered through the same angle ψ and the effective value of the cross section differs from the value corresponding to the angle ψ. This effect is quite significant for angles of scattering $< 10°$ where $d\sigma/d\Omega$ varies rapidly with ψ. For such small values of ψ, the intrinsic efficiency ϵ of the detector is a function of the distance r of the point of incidence of radiation on the front surface of the detector from the center of the surface,

$$\epsilon = \epsilon(r) . \tag{7}$$

Relative values of $\epsilon(r)$ are shown in Fig. 4, where $\epsilon(0)$ has been set as unity, while the small central dip in the efficiency curve, typical of a coaxial detector, may be disregarded without introducing appreciable error. It may also be assumed that for small angles $(< 10°)$ $\epsilon(r)$ is independent of the angle of incidence of photons, i.e., the usual paraxial geometry treatment has been assumed to be valid.

By introducing a Cartesian coordinate system with origin and source coincidental, $S(0,0,0)$, as illustrated in Fig. 5, we may show that, if a photon scattered at the point $(h,k,0)$ of the scatterer is incident at a point $(2l,y,z)$ of the detector, the angle of scattering is given by
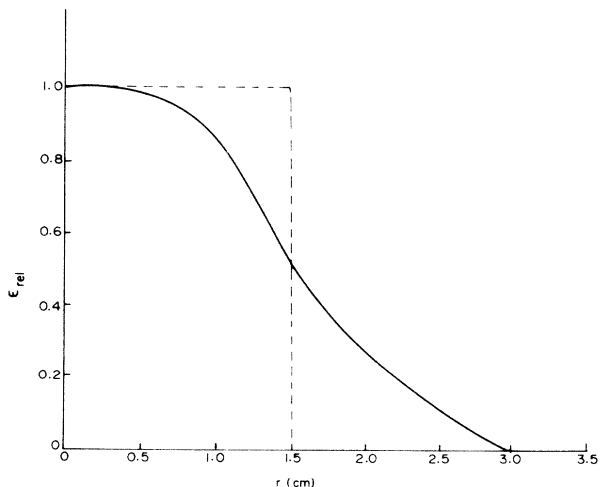
FIG. 5. Effect of the finite size of the detector on definition of the scattering angle ψ.

$$\cos\psi = \frac{h(2l-h)+k(y-k)}{(h^2+k^2)^{1/2}[(2l-h)^2+(y-k)^2+z^2]^{1/2}} ; \tag{8}$$

then the effective mean value $\bar{\sigma}_{hk}$ of the cross section is given by

$$\bar{\sigma}_{hk}\int_D \epsilon(y^2+z^2)^{1/2}dy\,dz = \int_D \sigma(\psi)\epsilon(y^2+z^2)^{1/2}dy\,dz , \tag{9}$$

where the subscript D indicates integration over the whole detector face. The value of $\bar{\sigma}_{hk}$ will differ from the nominal value of the cross section, σ_0, which corresponds to the angle of scattering ψ_0 given by

$$\cos\psi_0 = \frac{h(2l-h)-k^2}{(h^2+k^2)^{1/2}[(2l-h)^2+k^2]^{1/2}} . \tag{10}$$

In order to estimate the resultant error, substitution has been made of the theoretical values from the prescription of Kissel et al.[1] into the above equations. Since these values are only available for a few angles and since the cross sections vary rapidly with scattering angle in this region, a simple extrapolation procedure was developed to obtain values for any angle in the range by plotting $\sigma\psi^n$ against ψ, where n was chosen to be between 2 and 3 thereby making $\sigma\psi^n$ approximately constant (Fig. 6). Using this procedure it was found to be relatively easy to obtain cross-section values to within an error limit of $O(1\%)$.

The average value of $\bar{\sigma}_{hk}$ obtained in the above manner was finally extended over the entire scatterer by varying h

FIG. 4. Variation of the relative detector efficiency ϵ_{rel} as a function of the distance r of the point of incidence of radiation on the front surface of the detector from the center of the surface of the detector.
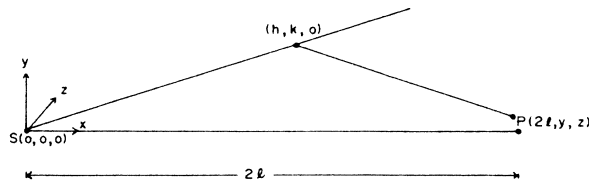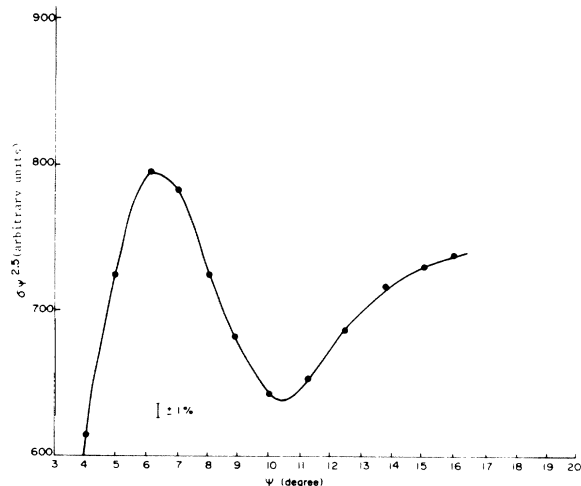
FIG. 6. An accurate interpolation of the differential coherent cross section based on predictions of Kissel, Pratt, and Roy.

(due to symmetry $\bar{\sigma}_{hk}$ is independent of k).

The estimated error in the cross section in the case of $\psi = 10°$ for Pb at 661.6 keV was, for instance, found to be $+7\%$ with an associated uncertainty of $\pm 2\%$. For $\psi > 20°$ the calculated error was within the error limits and explict correction was accordingly neglected. The estimate of error limits are based on the following considerations.

(i) Deviation of the formula of Kissel et al.[1] from actual cross-section values; an outer limit of 20% was assumed in accord with the variations reported in the values of other experimenters. In light of the claim of Kissel et al.[1] of an error in computation of $O(1\%)$ this estimate should be considered more than adequate.

(ii) Errors due to computation, finite angular grid size chosen for numerical integration, etc., for which an additional outer limit of 20% has been chosen.

If the actual active detector region is replaced by an idealized detector of width approximately equal to the full width at half sensitivity, viz., the width at 50% of the maximum response of the detector (say $r = 1.5$ cm), then essentially the same value for the estimated error is obtained. This simplified derivation has been used in all subsequent calculations. In Table I the factors required for correction of cross-section values at a scattering angle of 10° for Pb and Sn, arising from the finite lateral dimensions of the detector, are reproduced. For larger values of ψ, the factor is essentially 1.00.

Evaluation of the effect of the finite length of the detector has indicated that this correction may be neglected. Variation of the scattering angle ψ over the entire length of the detector is of the order of $\pm 0.1°$ for $\psi = 10°$. Taking the corresponding values of Kissel et al.[1] as in the previous case, it may be demonstrated that a resultant error in $d\sigma/d\Omega$ of the order of 0.1% might be expected.

TABLE I. Multiplicative correction factors for errors arising from the finite lateral dimensions of the detector.

E (MeV)	Sn	Pb
0.279	0.96±0.02	0.99±0.02
0.662	0.95±0.02	0.93±0.02

For other values of ψ the errors are of even smaller magnitudes. Similarly it may be demonstrated that the effects of finite source size are negligible.

E. The effect of variation of the efficiency of the detector with the position of the scattering element

Use of an auxiliary source has been widespread in measurement of cross sections, in order to eliminate explict dependence on efficiency. Although the inverse-square relationship has often been assumed, more-detailed investigations performed herein indicate substantial deviations and in particular over the scatterer surface.

The experiment was performed by moving the auxiliary source along lines of constant angle ranging from 0° to 60°, focused on a suitable reference point within the detector and measured from the horizontal line separating the primary-source position and the detector. The net auxiliary count rates n_c were recorded at suitable intervals along the lines of constant angles and graphs of $r_2^2 n_c$ versus r_2 constructed (Fig. 7). Deviations from a simple r_2^2 relation were found to be most marked for the smaller distances. Interpolated values of n_c for the various values of x as defined by Eq. (1) were obtained from the calibration graphs and introduced into the integral f as defined by Eq. (3).
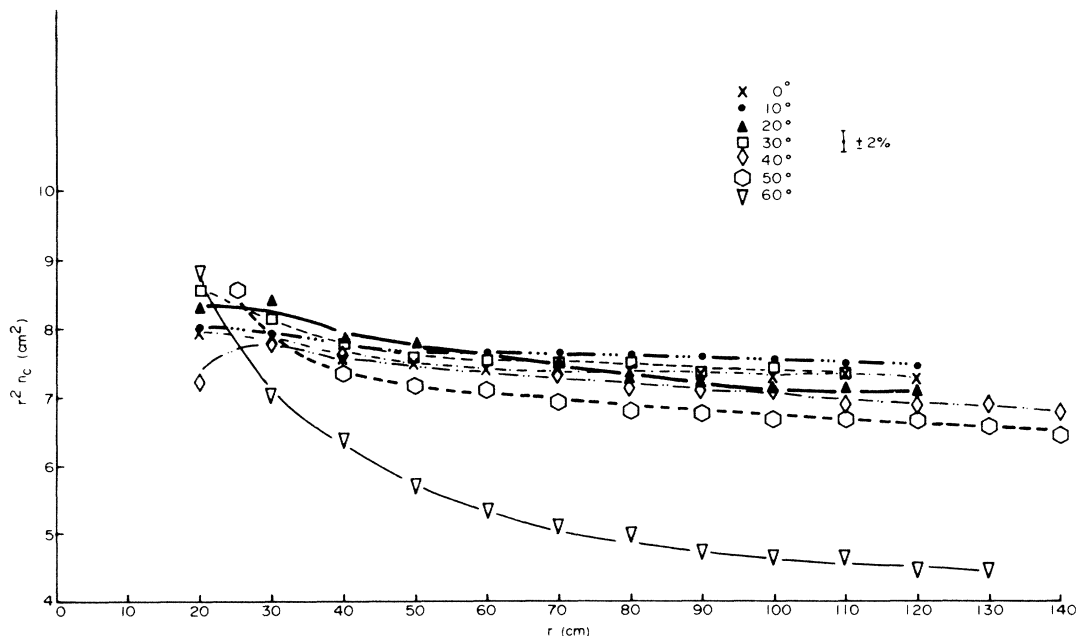

FIG. 7. Examination of departure from an inverse-square relationship as a function of distance from the detector along various lines of constant angle (as defined in the text).

F. The effective angle of scattering

Under suitable conditions of, for instance, well-resolved peaks one may determine the angle of scattering by noting the position of the incoherent peak. Assuming that the incoherent part of the spectrum peaks at the position corresponding to the free-electron Compton scattering then

$$\psi = \cos^{-1}\left[1 - \frac{1}{\alpha}\left[\frac{\Delta(h\nu)}{h\nu - \Delta(h\nu)}\right]\right], \tag{11}$$

where $\alpha = h\nu/m_e c^2$, $\Delta(h\nu)$ is the Compton shift in energy, $h\nu$ the energy of the incident photon, and $m_e c^2$ is the rest energy of the electron (0.511 MeV). Exact peak positions have been determined by assuming a Gaussian shape over the immediate peak region, of the form

$$y_i = Ae^{-b(x_i - c)^2}, \tag{12}$$

where y_i are the channel counts in a given channel x_i, A is a normalizing factor, and b and c are constants characteristic of the particular peak, representative of the full width at half maximum and the actual peak position, respectively.

The uncertainty in scattering angle is found to be dependent on the uncertainty in coherent and Compton peak positions $\Delta c'$ given by

$$\Delta c' = (\Delta c_1^2 + \Delta c_2^2)^{1/2}, \tag{13}$$

Δc_1 and Δc_2 being the uncertainty in the Compton and the coherent peak, respectively. Estimates of Δc have been obtained by considering the long-term stability of the electronics, statistical fluctuation in counting rates, etc. In this context electronic stability was monitored throughout the duration of the experiment utilizing a small ^{137}Cs source. Monitor readings remained consistently within 1% of the mean value.

G. Estimation of the photopeak intensity

In situations where the full-energy peak base line is comparable in extent to peak height substantial error may be introduced by erroneous delination of the background. We have developed a simple procedure for estimating full-energy peak counts by utilizing the fact that the primary radiation incident on the detector has the same shape as the coherently scattered peak. The background counts in the full-energy peak region were determined by fitting fourth- or fifth-order Lagrangian polynomials to data points which are distant enough from the peak region so that they do not include any significant component of the photopeak counts. The counts obtained by subtracting the background in this way were compared with the primary peak shape obtained previously. The fit was considered satisfactory only when all the points in the scattered peak when normalized agreed with the corresponding normalized primary full-energy points.

H. Source comparisons

One of the most important steps in the determination of the absolute value of the coherent-scattering cross section

involves the comparison of the strong primary source and the auxiliary source. Since the dynamic range of the detector system is usually inadequate to cope with a variation of counting rate by a factor of 10^5—10^6, it is often necessary to reduce the primary source strength in a predetermined manner, as for example, by interposing between the source and detector, a high-Z material such as lead, of known thickness. This particular procedure is however subject to appreciable errors arising from, in particular, multiple scattering within the attenuating media whose dimensions may exceed several mean-free-path lengths. Another method of securing reduction in primary source strength is to remove the source to a distance suitably far from the detector. However, this procedure too is subject to errors, primarily as a result of ground and air scattering, rendering an inverse-square relationship less accurate.

In the experiment reported herein source-intensity comparisons were performed by utilizing an additional source, intermediate in activity, I_2, between that of the primary source, I_1, and that of the auxiliary source, I_3. For the primary and intermediate sources placed at a suitably far, identical distance, so that dead-time effects remained small, the relative intensities were recorded as I_1/I_2. For the intermediate and auxiliary sources placed at an identical, conveniently near distance, dependent upon dead-time and positional uncertainty effects, the relative intensities were recorded as I_2/I_3. Thus the relative intensities of primary to auxiliary source were found from the relation

$$I_1/I_3 = (I_1/I_3)(I_2/I_3). \tag{14}$$

I. Effect of local curvature

Complete description of attenuation within the scattering media requires that allowance be made for local effects of scatterer curvature. In effect, correction for curvature will only arise for small-angle scattering where the angle $(\phi + \psi)$ approaches 90° and accordingly path lengths within the scatterer become large. From Fig. 8 it is clear that

$$\eta = 2r\cos\theta. \tag{15}$$

Writing $\rho = \eta_2/\eta_1$ one can show that

$$\left[1 - \frac{\eta_1^2}{4r^2}\rho^2(1 + \rho^2 + 2\rho\cos\psi)^{1/2}\right]$$

$$+ \frac{\eta_1\rho}{2r}(1 + \rho^2 + 2\rho\cos\psi)^{1/2} = \sin\psi(1 + \rho^2 + 2\rho\cos\psi). \tag{16}$$

This relation is a transcendental equation which can be solved by iteration, the initial value of path length η_2 being taken from the plane-geometry case.

Another effect of curvature is that the limits of integration imposed on the term f should be modified according to the relation
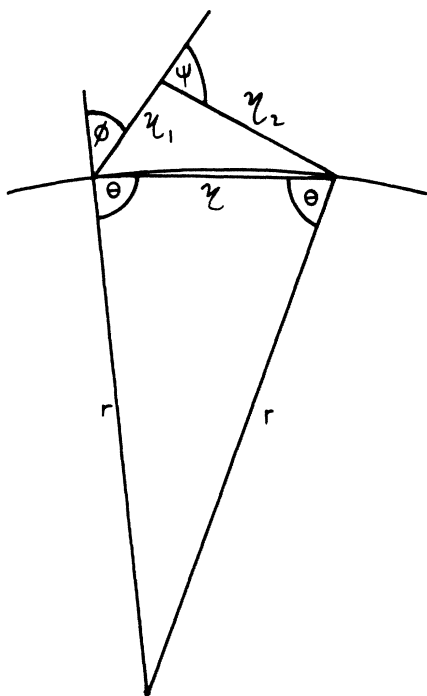
FIG. 8. Effect of local curvature on attenuation within the scattering media.

$$x_m = \frac{\sin\left[\frac{s}{l}\sin\psi\right]}{\sin\psi} , \qquad (17)$$

where s is the length of the scattering strip as measured along the arc. The deficit Δx between the limits of a plane geometry $x = \pm 0.5$ and that of x_m can be used as a correction term in the numerical integration procedure.

J. Purity of samples

X-ray fluorescence measurements showed that the purity of the tin and lead were in excess of 99% with no indication of any high-Z impurities.

IV. RESULTS AND DISCUSSION

In light of the foregoing discussions presentation will be made herein of differential coherent cross sections of uncertainty $O(5\%)$ within the range of scattering angles $10°-60°$.[20]

A. Estimation of error

Estimates of the sizes of individual error components (intended to represent estimates at the 95% confidence level) discussed in Sec. III are summarized in Table II.

To estimate the overall final uncertainty, the contributory errors are combined quadratically to obtain the root-mean-square error of the measurements, $\pm 6.5\%$ at $60°$; for $10°$ a possible error due to definition of angle of scattering may push the error limits to a maximum of $\pm 10\%$ whilst for other angles the error remains at $\pm 4.7\%$.

B. Comparison with experiment

Coherent differential cross sections have been obtained for a range of moderate angles for Sn and Pb and for the photon energies 279.2 and 661.6 keV. These values are reported in Tables III—VI inclusive of a comparison with predictions of Kissel et al. Since the scattering angles reported herein are not in exact accord with the tabulated values of the predictions of Kissel et al.,[1] interpolation has been carried out. The interpolated values have an estimated error of $\pm 1\%$ or less.

For scattering angles of $30°$ or less a source-to-detector separation of 2 m was found to be suitable. For scattering angles in excess of $30°$ a source-to-detector distance of 1 m was found to be more practically manageable. In order to ascertain that all dependences on the particular choice of distance had been adequately accounted for, some overlap of scattering angle was deliberately introduced. In particular, for the nominal scattering angle $30°$, measurements were repeated for both source-to-detector distances. No inconsistency has, within the limits of experimental error, been detected.

Although in studies of this type semilogarithmic pre-

TABLE II. Upper limits of the estimated percentage of errors arising from different correction factors.

Correction	95% confidence levels of estimated percentage errors
Efficiency measurements, $\Delta\epsilon$	± 2
Counting error	± 1
Background correction (excepting $\psi = 60°$)	± 2[a]
Finite scatterer thickness	± 1
Finite detector dimensions	± 2
Finite source dimensions	± 0.5
Source comparison measurements	± 1.5
Deviation from ideal geometry	± 2.0
Error in ψ (excepting $\psi = 10.5°$)	± 0.5
Multiple scattering	± 1.5

[a]The background correction at $\psi = 60°$ is estimated to be of the order of $(-5 \pm 2)\%$.

TABLE III. Coherent differential cross sections from experiment and theory. Photon energy, 279 keV; scattering element, Pb.

Nominal source-to-detector separation (m)	ψ (deg)	Experiment (b/sr)	Theory (b/sr)
2	10.5	12.0 ±1.2	16.0
2	20.2	3.12 ±0.16	3.25
1	24.8	1.64 ±0.08	1.75
2	29.6	1.17 ±0.06	1.21
1	29.8	1.15 ±0.06	1.19
1	34.4	0.760±0.038	0.860
1	39.2	0.545±0.027	0.596
1	44.1	0.398±0.020	0.398
1	48.5	0.295±0.015	0.276
1	59.0	0.122±0.008	0.125

TABLE IV. Coherent differential cross sections from experiment and theory. Photon energy, 279 keV; scattering element, Sn.

Nominal source-to-detector separation (m)	ψ (deg)	Experiment (b/sr)	Theory (b/sr)
2	10.5	3.09 ±0.31	3.80
2	20.2	0.850 ±0.043	0.900
1	24.8	0.408 ±0.020	0.435
2	29.6	0.243 ±0.012	0.238
1	29.8	0.246 ±0.012	0.232
1	34.4	0.136 ±0.007	0.140
1	39.2	85.9(−3)±4.3(−3)	94.0(−3)
1	44.1	70.6(−3)±3.5(−3)	69.0(−3)
1	48.5	57.9(−3)±2.9(−3)	55.0(−3)
1	59.0	30.7(−3)±2.0(−3)	33.0(−3)

TABLE V. Coherent differential cross sections from experiment and theory. Photon energy, 662 keV; scattering element, Pb.

Nominal source-to-detector separation (m)	ψ (deg)	Experiment (mb/sr)	Theory (mb/sr)
2	10.5	1.26 (3) ±0.13(3)	1.75(3)
2	20.2	0.310(3) ±0.016(3)	0.325(3)
1	24.8	0.133(3) ±0.007(3)	0.141(3)
2	29.6	72.0 ±3.6	75.0
1	29.8	77.7 ±3.9	74.0
1	34.4	45.5 ±2.3	49.0
1	39.2	33.6 ±1.7	34.6
1	44.1	23.4 ±1.2	24.9
1	48.5	16.7 ±0.8	18.7
1	59.0	9.19 ±0.60	9.30

sentation has been conventional, it is not, in our opinion the most suitable option. We have found that a better representation can be had by developing a crude relationship of the form

$$\sigma' \propto q^{-m} , \qquad (18)$$

where σ' is representative of the reduced differential coherent cross section

$$\sigma' = \frac{\sigma(\psi)}{\frac{1}{2}(1+\cos^2\psi)} , \qquad (19)$$

$\sigma(\psi)$ is the differential cross section, q is the momentum transfer, and m is some convenient number approximately between 2 and 4.

Herein x arguments, where $x = \sin(\psi/2)/\lambda(\overset{\circ}{A})$, rather than q arguments have been utilized. In Figs. 9—12 presentation has been made of the measured differential Ray-
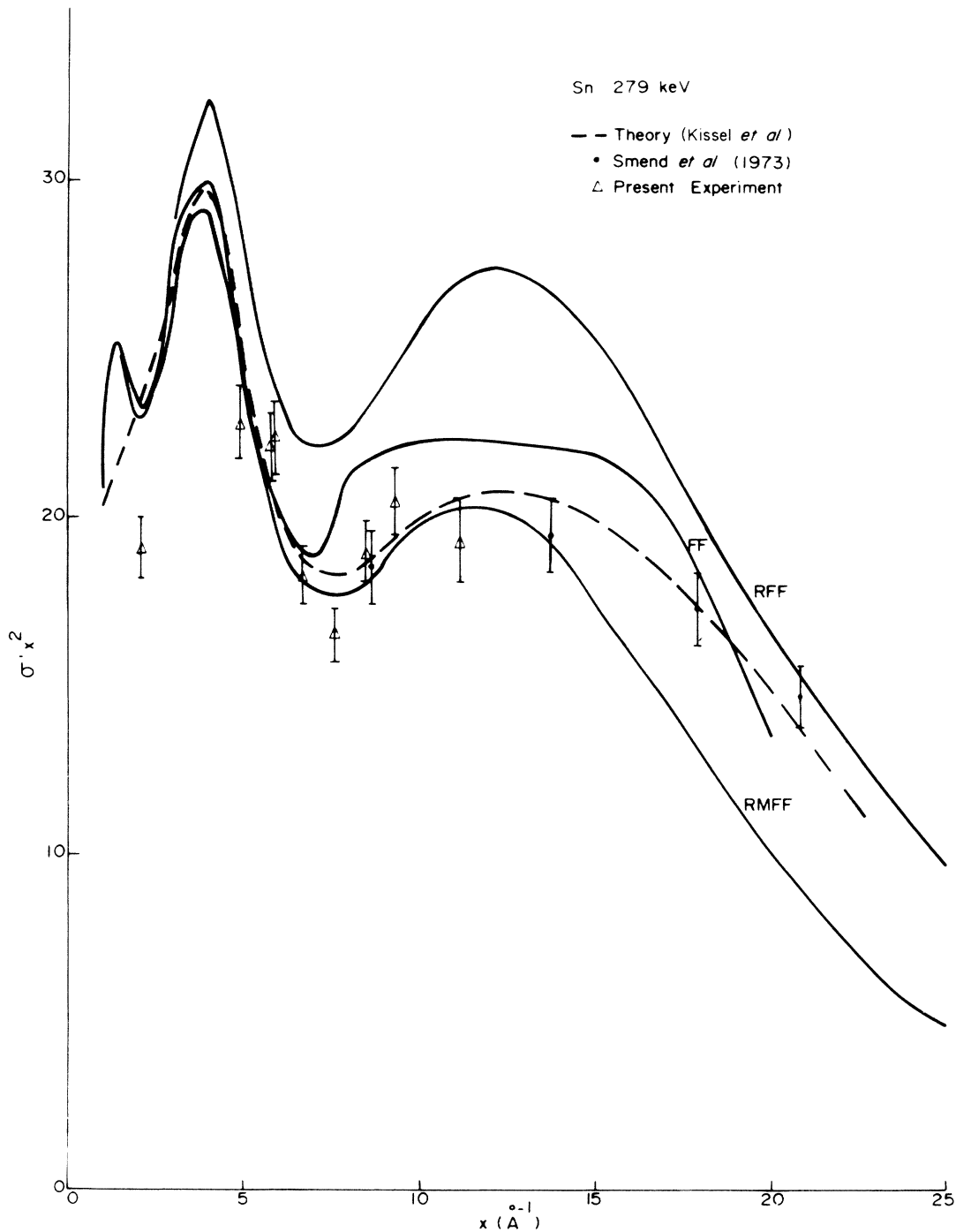
FIG. 9. Comparison of differential Rayleigh cross sections for Sn and 279.2-keV photons as predicted by FF, RFF, RMFF, and Kissel et al. with measured values [see Smend et al. (Ref. 25, 1973)].
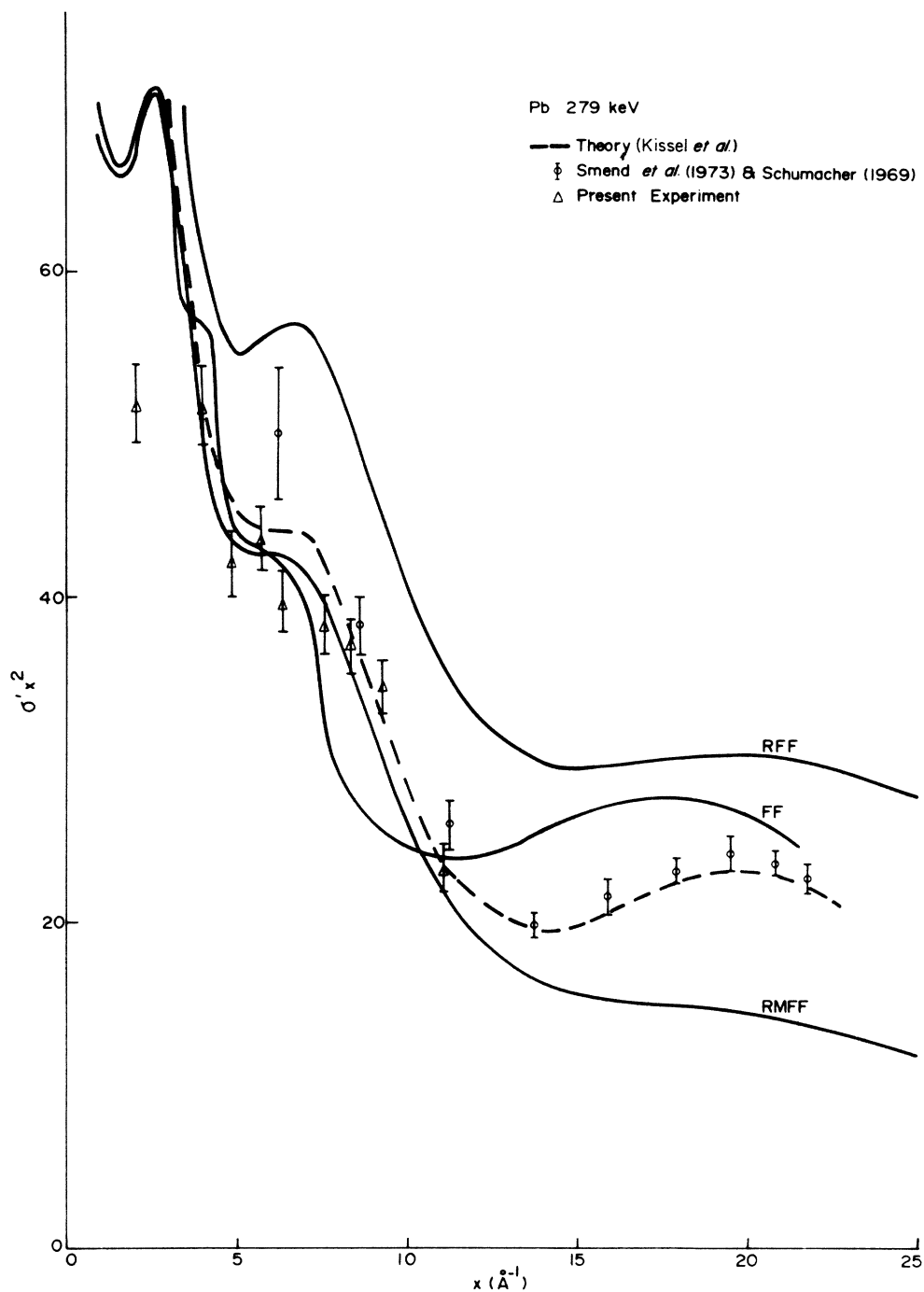
FIG. 10. Comparison of differential Rayleigh cross sections for Pb and 279.2-keV photons as predicted by FF, RFF, RMFF, and Kissel *et al.* with measured values [see Smend *et al.* (Ref. 25, 1973) and Schumacher *et al.* (Ref. 26, 1969)].

leigh cross sections for Sn and Pb for the photon energies 279.2 and 661.6 keV together with those determined from the Kissel-Pratt-Roy prediction, the form-factor (FF) formulation, the relativistic form-factor (RFF) formulation, and the modified relativistic form-factor (MRFF) formulation.

C. Observations

The following observations emerge clearly from the analysis.

(a) In general the experimental results overwhelmingly support the calculations of Kissel *et al.*; of the several
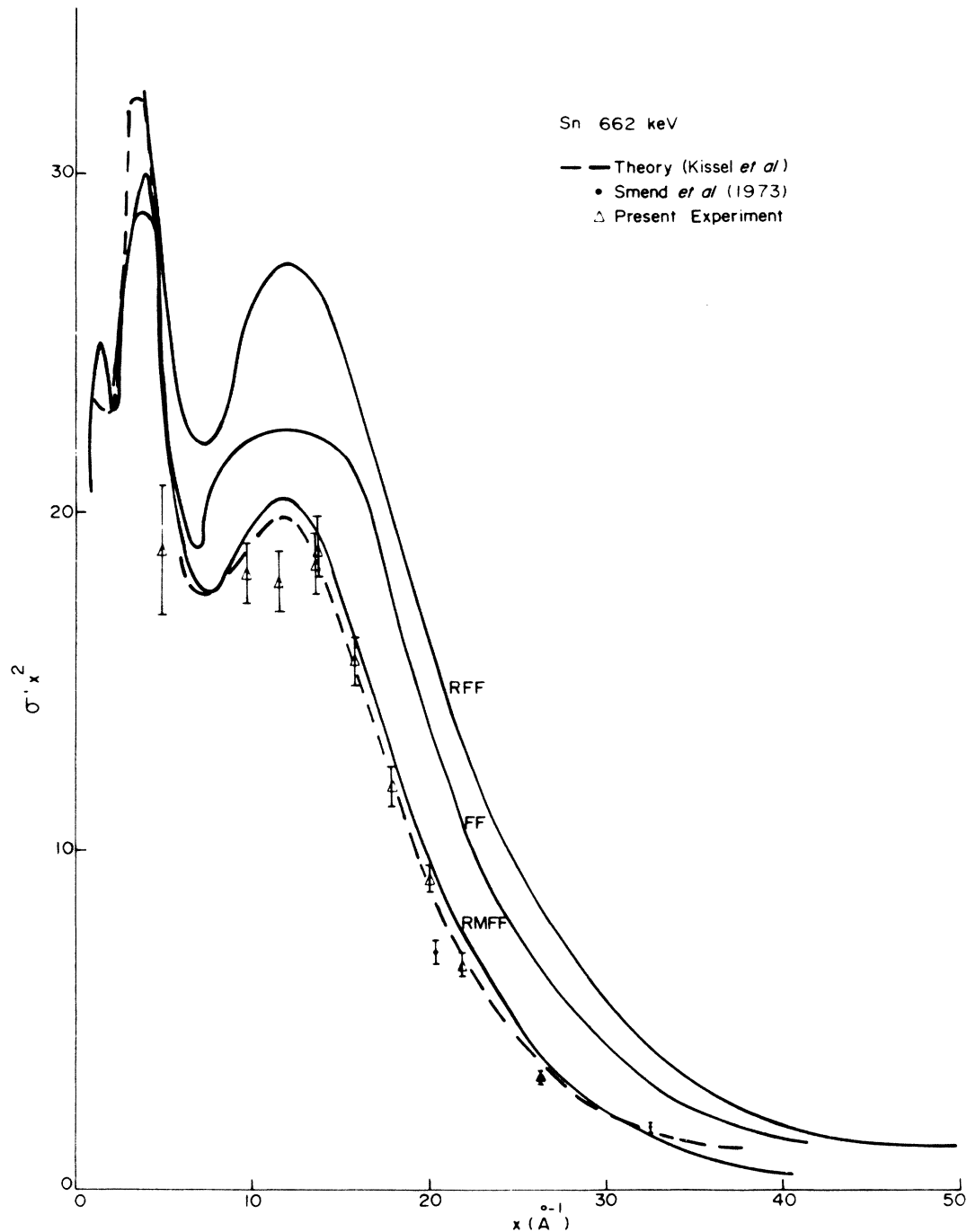
FIG. 11. Comparison of differential Rayleigh cross sections for Sn and 661.6-keV photons as predicted by FF, RFF, RMFF, and Kissel et al. with measured values [see Smend et al. (Ref. 25, 1973)].

form-factor formulations the modified form-factor predictions seem to be in closer agreement with the experimental results.

(b) Nevertheless, in many cases experimental data appear to bunch a few percent below the calculated values.

(c) It is difficult to point out any general trend in the values of the form-factor calculations excepting that the RFF data lie above those given by other formulations. More comprehensive analysis including other scattering elements at other energies (Bradley and Ghose[21]) have shown that even this trend is not universally true; the example of 59.54-keV photons scattered by Zn is a case in point. A coherent analysis would require more detailed individual studies.
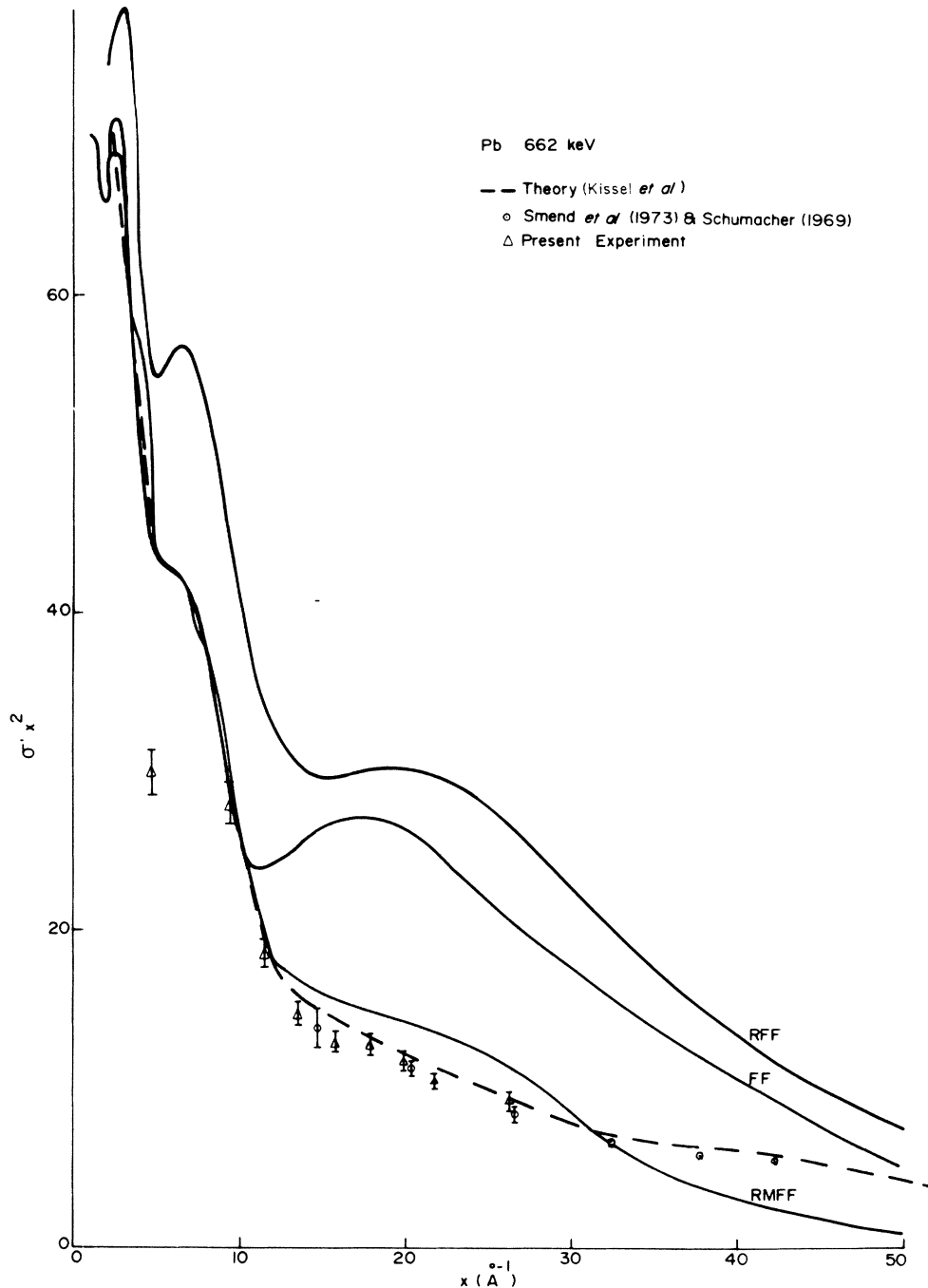
FIG. 12. Comparison of differential Rayleigh cross sections for Pb and 661.6-keV photons as predicted by FF, RFF, RMFF, and Kissel *et al.* with measured values [see Smend *et al.* (Ref. 25, 1973) and Schumacher *et al.* (Ref. 26, 1969)].

(d) The 10.5° scattering data systematically lie below the predictions of Kissel *et al.* the difference being of the order of 25%-.

D. Small-angle scattering deviations

Angular definition at small angles is a notable problem. At angles of 10.5° and less, a 1° change in ψ corresponds to an $O(25\%)$ change in σ; for smaller angles, changes are even more rapid. However, an error in ψ of $O(0.1°)$ is

the most that could possibly be justified, as discussed earlier. At other angles reported herein such fluctuations would have markedly less effect. In this particular connection one is also not sure how such rapid variations in cross sections would be reflected in the corresponding theoretical calculations. An additional factor to be considered is that for small q the location of the incoherent peak may not coincide with the free-electron Compton peak.

Note is taken of similar variations occurring wherever

TABLE VI. Coherent differential cross sections from experiment and theory. Photon energy, 662 keV; scattering element, Sn.

Nominal source-to-detector separation (m)	ψ (deg)	Experiment (mb/sr)		Theory (mb/sr)
2	10.5	0.357(3)	±0.036(3)	0.450(3)
2	20.2	65.5	±3.3	68.8
1	24.8	38.0	±1.9	42.0
2	29.6	24.6	±1.2	25.0
1	29.8	24.8	±1.2	24.0
1	34.4	13.9	±0.7	13.9
1	39.2	7.51	±0.40	7.65
1	44.1	4.24	±0.21	4.30
1	48.5	2.38	±0.12	2.50
1	59.0	0.720	±0.047	0.790

$x^m\sigma'$ varies rapidly with x, although the degree of variation is smaller. There is therefore a need to obtain further confirmation of σ for small angles.

Examination has been undertaken of the experimental data of several other groups who have used high-resolution detection systems for other energies and scatterers. A definite trend is indicated with which the present findings are in accord. Figure 13 reveals a tendency for experimental data to lie, in the main, below that of the predictions of Kissel et al. However, except for the smaller-angle data the deviations tend to remain within expected experimental errors and a general improvement in agreement is found as the scattering angle increases. That the deviations might be explained on the basis of systematic or normalization errors seems unlikely since the trend is reflected in the results of the majority of data included in the analysis. The experimental findings of

Chitwattanagorn et al.[22] and Taylor et al.[23] have not been utilized as the data has been shown to be subject to rather large fluctuations, finding little accord with the data of many other workers. Taylor et al.[24] have recently indicated that substantial discrepancies have been found to exist in the previously reported data of Chitwattanagorn et al. but the new findings have not been tabulated as such.

E. Discussion

The surface-of-revolution geometry as utilized herein is capable of providing accurate $O(5\%)$ coherent-scattering cross-section data for scattering angles of 10° and above; modifications allowing measurements in excess of 90° have been discussed elsewhere.[19] The method is potentially valuable for measurements of cross sections of low-Z
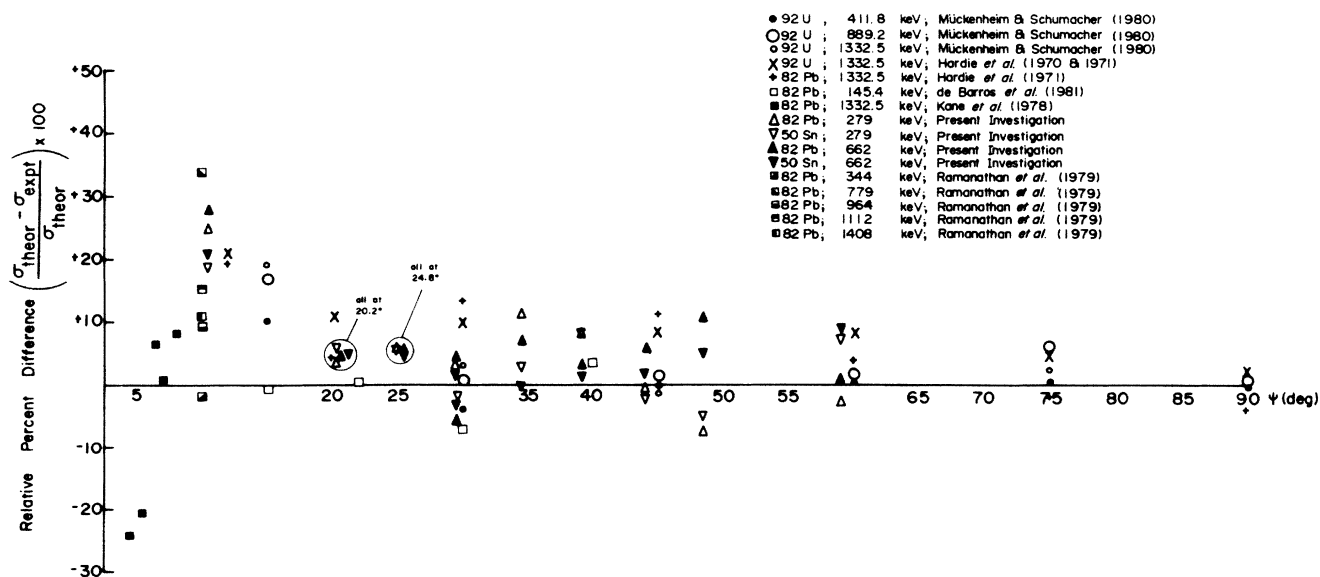

FIG. 13. Comparison, as a function of scattering angle ψ, of the prediction of Kissel et al. with differential Rayleigh cross sections based on the measurements of several experimenters using high-resolution detection systems. [See Mückenheim and Schumacher (Ref. 27), Hardie et al. (Refs. 28 and 29), de Barros et al. (Ref. 30), Kane et al. (Ref. 31), and Ramanathan et al. (Ref. 32)].

scatterers; pilot studies conducted in this laboratory have, for instance, indicated that for aluminum and 661.6-keV photons a coherent peak containing sufficient counts for the attainment of differential coherent cross sections of $O(10\%)$ uncertainty can be had for counting times of the order of several hours. In this context it is to be noted that measured data for elements lighter than copper are practically nonexistent for the range of energies provided by isotopic sources.

Whilst present measurements support the Kissel-Pratt-Roy predictions further studies are required for the angles of scattering less than 10°. Measurements in this region would require the use of a multifilter technique in order to reduce the associated problems of a sample-dependent background.[19] On the theoretical side since there is a greater dependence upon higher shells at low momentum transfers, exact numerical calculations, though involving considerable computation time, would be worthwhile.

[1]L. Kissel, R. H. Pratt, and S. C. Roy, Phys. Rev. A 22, 1970 (1980).
[2]A. Nath, Trans. Bose Res. Inst. 29(2), 51 (1966).
[3]A. M. Ghose, in Proceedings of the First International Symposium on Radiation Physics, edited by A. M. Ghose, D. V. Gopinath, J. H. Hubbell, and S. C. Roy, Natl. Bur. Stand. (U.S.) Spec. Publ. No. 461 (U.S. GPO, Washington, D.C., 1974), p. 47.
[4]J. H. Hubbell, Wm. J. Veigele, E. A. Briggs, R. T. Brown, D. T. Cromer, and R. J. Howerton, Phys. Chem. Ref. Data 4, 471 (1975).
[5]J. H. Hubbell and I. Øverbo, Phys. Chem. Ref. Data 8, 69 (1979).
[6]W. Franz, Z. Phys. 95, 652 (1935); 98, 314 (1936).
[7]D. Schaupp, M. Schumacher, F. Smend, P. Rulhusen, and J. H. Hubbell, J. Phys. Chem. Ref. Data 12, 467 (1983).
[8]G. E. Brown and J. B. Woodward, Proc. Phys. Soc. London Sect. A 65, 988 (1952).
[9]G. E. Brown, R. E. Peierls, and J. B. Woodward, Proc. Phys. Soc. London Sect. A 227, 51 (1954).
[10]S. Brenner, G. E. Brown, and J. B. Woodward, Proc. Phys. Soc. London Sect. A 227, 59 (1954).
[11]G. E. Brown and D. F. Meyers, Proc. R. Soc. London Ser. A 234, 987 (1955).
[12]G. E. Brown and D. F. Meyers, Proc. R. Soc. London Ser. A 242, 89 (1957).
[13]H. Cornille and M. Chapdelaine, Nuovo Cimento 14, 1386 (1959).
[14]W. R. Johnson and F. D. Feiock, Phys. Rev. 168, 22 (1968).
[15]W. R. Johnson and F. D. Feiock, Phys. Rev. 187, 39 (1969).
[16]Lin Chien-Ping, Cheng Kwok-Tsang, and W. R. Johnson, Phys. Rev. A 11, 1946 (1975).
[17]W. R. Johnson and Cheng Kwok-Tsang, Phys. Rev. A 13, 692 (1976).
[18]L. Kissel and R. H. Pratt, Phys. Rev. Lett. 40, 387 (1978).
[19]A. M. Ghose and D. A. Bradley, Indian J. Phys. 58A, 71 (1984).
[20]D. A. Bradley, Ph.D. thesis, Universiti Sains Malaysia, Penang, Malaysia (unpublished).
[21]D. A. Bradley and A. M. Ghose, Internal Report, School of Physics, Universiti Sains Malaysia, Penang, Malaysia, March, 1985 (unpublished).
[22]W. Chitwattanagorn, R. B. Taylor, P. Teansomprasong, and I. B. Whittingham, J. Phys. G 6, 1147 (1980).
[23]R. B. Taylor, P. Teansomprasong, and I. B. Whittingham, Aust. J. Phys. 34, 125 (1981).
[24]R. B. Taylor, P. Teansomprasong, and I. B. Whittingham (unpublished).
[25]F. Smend, M. Schumacher, and I. Borchert, Nucl. Phys. A213, 309 (1973).
[26]M. Schumacher, Phys. Rev. 182, 7 (1969).
[27]W. Mückenheim and M. Schumacher, J. Phys. G 6, 1237 (1980).
[28]G. Hardie, W. J. Merrow, and D. R. Schwardt, Phys. Rev. C 1, 714 (1970).
[29]G. Hardie, J. S. De Vries, and Chiang Chwan-Kang, Phys. Rev. C 3, 1287 (1971).
[30]S. de Barros, J. Eichler, M. Gaspar, and O. Goncalves, Z. Naturforsch. 36A, 595 (1981).
[31]P. P. Kane, G. Basavaraju, J. Mahajani, and A. K. Priyadarsini, Nucl. Instrum. Meth. 155, 4671 (1978).
[32]N. Ramanathan, T. J. Kennett, and V. V. Prestwich, Can. J. Phys. 57, 343 (1979).